Comparisons of Quantitative Susceptibility Mapping (QSM) by using restricted oversampled spatial unit dipole field

Mai Murashima[1], Tomohiro Ueno[1], and Naozo Sugimoto[1]

[1]Human Health Science, Graduate School of Medicine, Kyoto University, Kyoto, Japan

Introduction: Quantitative Susceptibility Mapping (QSM) provides a distribution of tissue magnetic susceptibility differences by solving an inverse problem of perturbed static magnetic field. The perturbed magnetic field can be approximated in first order by a spatial convolution of the magnetic susceptibility distribution with a spatial unit dipole field. The dipole field decays with the cube of the distance ($\propto r^{-3}$) but its effect on the magnetic field becomes a slow decaying function of the distance ($\propto r^{-1}$) since larger volume ($4\pi r^2 \Delta r$) has to be included into calculation at longer distance. Therefore, the inverse problem has to be solved in infinite range although measured magnetic field is limited in FOV. To limit the calculation within FOV, various methods for background magnetic field removal were proposed [1-3]. Even after the inverse problem is restricted within the FOV, it is a severe burden for a computer to deconvolve the susceptibility distribution with the long ranged spatial dipole field in the spatial domain. On the other hand, near its origin the dipole field becomes larger and changes very much within a short distance. These can be understood by the fact that the magic angle cones of the dipole field extend from the origin and the field value changes its sign across the cone. Therefore, a digitally sampled spatial dipole field does not satisfy Laplace's equation, though continuous one does. This difference between the continuous field and the digitally sampled one produces errors in the deconvolving process. In this study, we performed numerical simulations taking into account partial volume effects, and we found the minimum size of the dipole field for the deconvolution and compared susceptibility distributions by using dipole fields with various oversampling factors.
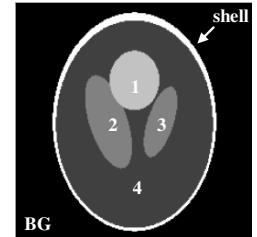

Fig1: Shepp-Logan phantom $((32\times7)^3$, z=113, χ_1:0.3ppm, χ_2, χ_3:0.2ppm, χ_4:0.1ppm, shell:1ppm, BG:0ppm)

Methods

Relative magnetic field difference including partial volume effects: A 3D Shepp-Logan phantom was created at the matrix size of $(32\times7)^3$. The susceptibility values (χ_i) of prolate spheroids were set to 0.3, 0.2, 0.2, 0.1, and 1 ppm, and the background was zero (Fig.1). A relative magnetic field difference (δ_B) was calculated by convolving with the spatial unit dipole field $(31\times7)^3$. Then δ_B in the regions corresponding to the shell (1ppm, bone) and the background (0ppm, air) was set to 0 so as to simulate MRI measurements. The δ_B distribution was downscaled to $(32)^3$ by averaging every $(7)^3$ voxels and added a white Gaussian noise to have SNR = 20.

Background field removal: The filtering using the spherical mean value property of harmonic functions was performed on the input δ_B with a sphere of diameter 9 voxels. After removing the background, the only region of 5 voxels inside from the measured δ_B was extracted for later processing of QSM.

Susceptibility estimation: Since our numerical phantom had no susceptibility anisotropy, we employed the multiple orientation method [4] to solve the inverse problem of the measured δ_B distribution. The δ_B distributions of three different angles (0°, 30°, and 60°) on the slice plane between the phantom and the main magnetic field were calculated. In order to estimate the susceptibility distribution in the spatial domain, the dipole fields with different diameters (D_d = 5-27 voxels) and with 4 different oversampling factors (n_{os} = 1, 3, 5, 7) were used. For each prolate spheroid, mean susceptibility (χ_{mi}) and its SD were calculated only in the region corresponding to the homogeneous part of the phantom and the relative mean susceptibilities to χ_{m4} ($\Delta\chi_{mi} = \chi_{mi} - \chi_{m4}$) were used for evaluation.

Oversampled dipole field: Each voxel was divided into $n_{os}{}^3$ isocubic subvoxels and the dipole field at each subvoxel was averaged within the voxel to be the oversampled dipole field of the n_{os} oversampling factor.
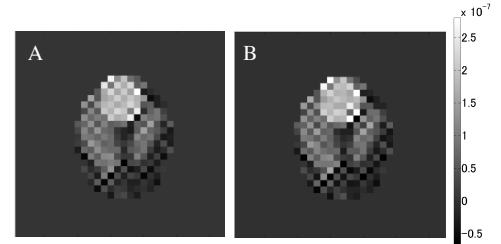

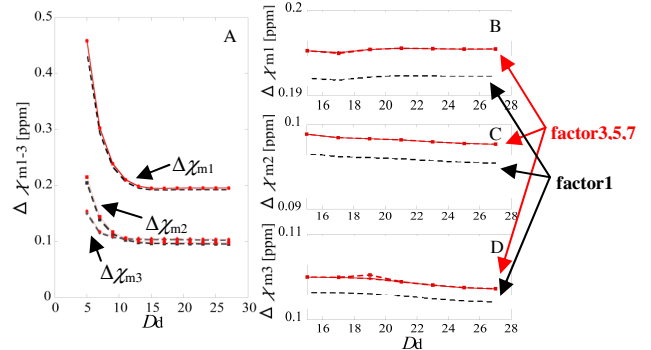Fig2: comparison of susceptibility estimations (z=17, D_d=27, A: n_{os} = 1, B: n_{os} = 3)

Fig3: (A) D_d dependences of $\Delta\chi_{m1-3}$, (B,C,D) blowups of A.

Results and Discussion: In Fig2, the calculated susceptibility distributions are shown and no large streaking artifact exists. D_d dependences of $\Delta\chi_{m1-3}$ with different n_{os} are shown in Fig3A. The $\Delta\chi_{m1-3}$ decrease as D_d becomes larger and reach constant values around D_d = 17, though $\Delta\chi_{m3}$ shows a different dependence and an overestimated value. Since the region3 has the smallest area (Fig1), fewer voxels may cause this deviation but this is left for later study. Therefore, D_d can be restricted to 21 with enough accuracy (differences of $\Delta\chi_{m1-3}$ from χ_{1-3} - χ_4: ~ 10^{-9}, SDs of χ_{m1-3}: ~ 10^{-8}). In Fig3B-D, differences of $\Delta\chi_{m1-3}$ between the oversampling scales n_{os} above D_d = 15 are shown. $\Delta\chi_{m1-3}$ with n_{os} = 3, 5, 7 show almost same values. This can be explained by that smaller subvoxel contributions were averaged out at the same size of voxel. $\Delta\chi_{m1-3}$ with n_{os} = 3, 5, 7 are higher than the n_{os} = 1 values and $\Delta\chi_{m1,2}$ with higher n_{os} are closer to the true values. Since the dipole field with $n_{os} \geq 3$ has smaller absolute value near its origin than one with n_{os} = 1, this difference may enhance calculated susceptibilities.

Conclusion: The diameter D_d = 21voxels of the spatial unit dipole field is sufficient for estimating a susceptibility distribution. The oversampled spatial unit dipole field (n_{os} = 3) is sufficient for observing effects on the susceptibility estimation and its validity needs further study.

References: [1] L Li et al. J. Magn. Reson. 148 (2001) 442-448. [2] F. Schweser et al. NeuroImage 54 (2011) 2789-2807. [3] T. Liu et al., NMR Biomed. 24 (2011) 1129-1136. [4] T. Liu et al. MRM 61 (2009) 196-204.